B-1.7 Impact assessment of global warming on the change of local climate with a local climate model including a forest ecosystem model

Contact person Hiroaki Kondo
Head
Atmospheric Environment Division
Environmental Assessment Department
National Institute for Resources and Environment
16-3, Onogawa, Tsukuba, Ibaraki, 305-8569, Japan
Tel:+81-298-61-8363 Fax:+81-298-8358
E-mail p1785@nire.go.jp

Total Budget for FY1997-FY1999 11,876,000 Yen (**FY 1999**; 3,956,000 Yen)

Abstract
The net ecosystem production (NEP) at Takayama forest was parameterized with temperature, available photosynthetic active radiation (APAR), and leaf area index (LAI). The variation of NEP due to temperature rise and change of APAR was estimated throughout a year. The distribution of CO_2 concentration and its time variation over central part of Japan was calculated for three days to check the parameterization based on Takayama data. The variation of NEP due to change of cloud amount in the area was also estimated.

Key words Deciduous forest, CO_2 concentration, Local climate model

1.Introduction

Due to the global climate change, it is apprehended that what kind of local effect appears in East Asia region and Japan. The possibility of the effect in which the human activity changed the land use by farming and industrialization on the climate system in local to regional scale has also been pointed out. The forest ecosystem plays an important role both for water and carbon cycles not only in global scale but in local scale. Because the ecosystem is various and diverse, there are many indefinite parts. In the present study, a model of forest ecosystem is developed on the basis of long-term observation data in a cool temperate broad-leaved deciduous forest of Japan, and the evaluation of the impact due to climatic change in the local scale is tried.

2.Research objective

In the present study, a sub-model of forest ecosystem is developed based on the long-term observation of the carbon dioxide and energy budget in a cool temperate broad-leaved deciduous forest in Japan. The impact of the variation of some climate parameters on the forest ecosystem is evaluated in the local scale.

3.Research method

Long-termed observation of CO_2 flux between a forest ecosystem and atmosphere has been performed at a tower on a ridge of 1420m height at Takayama since 1993 (Takayama site). A sub-model to calculate the uptake and release rate of CO_2 from the ecosystem was developed with the long-term data and vegetation map of Japan. The anthropogenic CO_2 source was also mapped. These sub-model and data were introduced in a local climate model. The sensitivity of NEP on temperature and APAR was investigated.

4.Results

4.1. Parameterization of evaporation and CO_2 uptake from various land surfaces

The evaporation from land surfaces was expressed as follows.

$$E = \rho \frac{G_a G_s}{G_a + G_s}\left(q^*(T_s) - q\right) \qquad (1)$$

Here, ρ is the air density, $q^*(T_s)$ is the saturation specific humidity for the surface temperature T_s. q is the specific humidity of the air, G_a is the efficiency of the sensible heat exchange (= C_H U), and G_s is the canopy conductance. The CO_2 uptake rate A was expressed as a function of the solar radiation I (W m^{-2}) and the air temperature T (℃) as follows.

$$A = \frac{bI}{1+aI} - R \qquad (2)$$

$$R = R_{25} Q^{\frac{T-25}{10}} \qquad (3)$$

Here, R is the CO_2 release rate at night, R_{25} (=0.078 $mgCO_2\ m^{-2}s^{-1}$) is the value of R at the air temperature 25 ℃, and Q (= 2) is a coefficient. Parameters G_s, a, and b were given by Schulze et al. (1994) in Table 1.

Table 1. Values of G_s, a, and b for various vegetative covers.

No.	Land use	G_s mm s^{-1}	a J^{-1} s m^2 $\times 10^{-4}$	b $mgCO_2\ J^{-1}$ $\times 10^{-3}$
1	Shrub	9.4	6.80	0.79
2	Evergreen conifers	20.6	6.80	1.71
3	Deciduous conifers	11.4	6.80	0.95
4	Deciduous broad leaf trees	20.7	6.80	1.72
5	Evergreen broad leaf trees	12.1	6.80	1.01
6	Mixed forest	13.8	6.80	1.15
7	Temperate grassland	23.0	6.80	1.92
8	Bog	5.0	6.80	0.42
9	Arable cropland	32.5	6.80	2.70
10	Others	25.1	6.80	2.08
11	Urban	--	--	--
12	Water	∞	--	--

4.2 CO_2 emission from anthropogenic activities

The data were mapped on 1/8° (in longitude) × 1/12° (in latitude), covering all of Japan on an hourly basis and providing monthly averages. Total anthropogenic emission was categorized into 7 classes: large plant facilities, small plant facilities (including small firms), offices, residences, motor vehicles, ships, and aircraft. Most CO_2 emission comes from industrial stationary sources, and these data were based on the database of the Japan Environmental Agency and the Ministry of International Trade and Industry. The data used here were limited to those from combustion of fossil fuels and cement kilns. Offices and residences include the emission from commercial and residential areas. Emission from motor vehicles was estimated from the amount of traffic, car type, and driving mode. Emission from ships was estimated from the total number of ships anchoring at the port. Emission from aircraft was

estimated by the landing and take-off cycle at the commercial airport alone. The total amount summarized here is 6.6% less than the total emission of CO_2 from Japan in 1994 (e.g., Agency of National Resources and Energy, 1999). The variation of total emission all over Japan in August is shown in Fig.1.

Effective stack height was considered for large emission stacks which exhaust heat above 10^6 cal s^{-1}. The emission from these stacks was treated individually, and their plume rise was estimated by the CONCAWE's equation (Brummage, 1968).

$$\Delta H = 0.175 Q_H^{\frac{1}{2}} u^{-\frac{3}{4}} \qquad (4)$$

Here, ΔH, Q_H, and u are plume rise, exhaust heat, and wind velocity at the actual stack height, respectively. CO_2 emission from these stacks was introduced in the grid, including effective stack height. Other sources were set at 10m above the ground.

4.3 Simulation of the daily variation of CO_2 concentration in central part of Japan

CO_2 concentrations at 30m above the surface calculated for Jul.23 to 25 in 1997 at Takayama is shown in Fig.2. In the figure, observed values of CO_2 are also shown. Though the simulation is very primitive, there are both similar and contradicting characteristics between the results of observations and calculations. For example, the maximum concentration of CO_2 was not attained just before sunrise but at midnight, both in calculations and observations. There was a steep decrease and recovery of CO_2 concentration just after sunrise in the observation. As a whole the amplitude of the daily variation was similar and the parameterization of the ecosystem seemed to be good.

4.4 Gross primary production and net ecosystem production estimated by the eddy covariance method

The fluxes of sensible heat, water vapor, and CO_2 have been measured by the eddy covariance method since 1998 summer at Takayama site. Fluctuations of wind and temperature are measured by a three-dimensional sonic anemometer-thermometer (model DAT-600, KAIJO), at 25.0 m on a 27 m tower. Fluctuations of CO_2 and water vapor concentrations are measured by a closed-path type infrared gas analyzer (model LI-6262, LI-COR). Leaf area index LAI have been measured since 1995 by the attenuation of the photosynthetic active radiation in the canopy, and by a plant canopy analyzer (model LAI-2000, LI-COR).

Figures 3 (a) to (e) show the seasonal and year-to-year changes in LAI. Leaf emergence began around April 30 (DOY 120) in 1998, and May 20 (DOY 140) in 1999. There was a clear shift in the growing period by about 20 days. Temperature in early spring is expected to be the most important factor for leaf emergency, and the accumulated temperature is often used to interpret the warmth in spring. Curves in Fig.3 show the results of calculation expressing the seasonal change in LAI based on an empirical equation using the accumulated temperature (> 5 ℃) in spring.

Relationship among NEP, GPP, and R is expressed as follows.

$$NEP = GPP - R \qquad (5)$$

Figure 4 shows a relation between R (symbols) and the nighttime air temperature T estimated by the nighttime CO_2 flux measurement. Data in the neutral conditions were used here in order to avoid methodological problems, which often occurred in stable night. The curve in Fig.4 shows the relation between R and T expressed as follows.

$$R = R_{10} Q^{\frac{T-10}{10}} \qquad (6)$$

Here, Q = 2.57 and R_{10} = 0.173 mol m^{-2} day^{-1} were determined by regression (r^2 = 0.48).

The daily value of GPP was calculated by GPP = NEP + R from 1998 to 1999, where daily NEP was estimated by the flux measurement. In this study, GPP was parameterized by the daily absorbed photosynthetic active radiation APAR as follows.

$$GPP = \frac{P_{max} \cdot APAR}{\frac{P_{max}}{\phi} + APAR} \qquad (7)$$

Here, P_{max} is the maximum level of the GPP-APAR curve (maximum canopy photosynthesis), and ϕ is its initial slope (light use efficiency). From further analysis, a linear relationship had been found between semimonthly determined P_{max} and LAI,

$$P_{max} = 0.439\,(LAI-0.6)+0.0645, \quad (r^2 = 0.62) \qquad (8)$$

while ϕ was generally constant throughout the growing period. (0.0427 mol-CO_2/mol-photon).

Daily value of NEP was calculated by Eqs. (5), (6), (7), and (8) as a function of T, APAR, and LAI. Figure 5 shows the seasonal changes in observed and calculated NEP, and calculated GPP and R.

Table 2 shows the sensitivity of the annual CO_2 budget of the forest to the changes in the meteorological conditions, such as the air temperature and the solar radiation. Case 0 is the calculated annual GPP, R, and NEP based on the temperature and the radiation of the normal year. Case 1 is the result when the solar radiation increased 10 % throughout the year. In this case, NEP increased 17.3 % with the increase in GPP. Cases 2 and 3 are the results when the solar radiation decreased in the rainy season from June to July (Baiu). In case 2, the solar radiation decreased 10 % from 1st June to 31st July. In case 3, the solar radiation decreased 50 % from 1st to 14th July. The cumulative solar radiation of case 2 from June to July is equivalent to that of case 3. Table 2 shows that the decrease in NEP in case 3 was more remarkable (-11.9 %) than that in case 2 (-7.8 %). The decrease in the summer solar radiation was quite sensitive to the annual NEP.

Cases 4, 5, and 6 show the sensitivity of NEP to the air temperature. Case 4 shows the result when the air temperature increased 1 ℃ throughout the year. In this case, GPP increased (+4.0 %) with the increase in the growing period (+5 days). However, the increase in R throughout the year was so significant (+9.9 %) that the annual NEP decreased (-10.7 %) after all. In case 5, the air temperature increased 1 ℃ before the growing period (spring), and in case 6, the temperature increased 1 ℃ from July to August (mid-summer). Table 2 shows that the higher air temperature in spring (case 5) caused the increase in NEP (+10.2 %) with the increase in the growing period(+5 days). While the higher temperature in mid-summer caused the increase in R (+3.9 %) and the decrease in NEP (-9.6 %).

4.5 Impact of cloud amount change

The impact of cloud amount change from 0 to 0.4 was investigated with local climate model which was the same model introduced in 4.3 as an example of climate change. The results

showed temperature decrease of 0.17 ° C and 10% reduction of NEP averaged over the central part of Japan in summer days.

Table 2. Sensitivity of GPP, R, and NEP to the solar radiation and the air temperature.

Case	Solar radiation (%)	Temperature (℃)	GPP (%)	R (%)	NEP (%)
0	0 (normal year)	0 (normal year)	0.0	0.0	0.0
1	+10 (throughout year)	0	+4.9	0.0	+17.3
2	-10 (two months in Baiu)	0	-2.2	0.0	- 7.8
3	-50 (two weeks in Baiu)	0	-3.4	0.0	-11.9
4	0	+1 (throughout year)	+4.0	+9.9	-10.7
5	0	+1 (before the growing period)	+4.0	+1.5	+10.2
6	0	+1 (two months in summer)	0.0	+3.9	- 9.6

5.Conclusion

The model results indicated that NEP deeply depends on the ambient temperature through the activity of respiration. The season of temperature change is also important. As a whole, high temperature causes to reduce NEP, but that in spring is increase NEP due to increase of growing period.

References

Agency of National Resources and Energy, 1999: *Energy 2000*, Denryoku shinpou-sha, 271pp. (in Japanese).

Brummage, K.G., 1968: The calculation of atmospheric dispersion from a stack, *Atmos. Environ.*, **2**,197-224.

Schulze et al., (1994): Relationships among maximum stomatal conductance, ecosystem surface conductance, carbon assimilation rate, and plant nitrogen nutrition. Ann. Rev. Ecol. Syst., 25: 629-660.

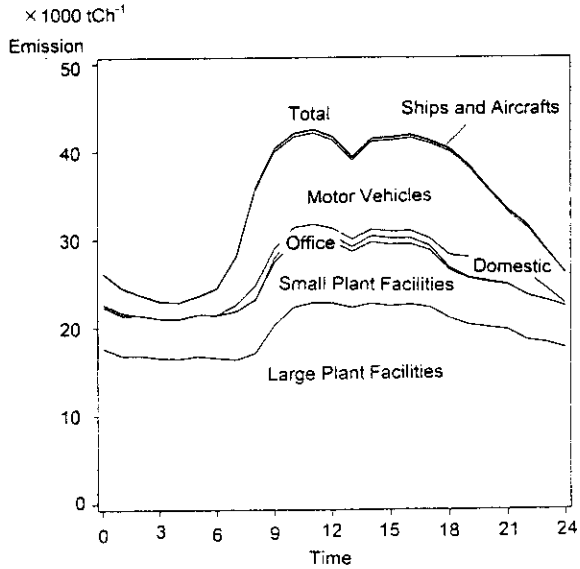

Fig.1 Time variation of total CO_2 emission all over Japan in August

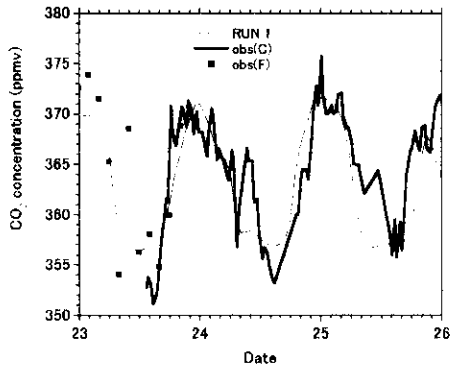

Fig.2 The daily variaition of CO_2 concentration at Takayama. Square is the observation by flask sampling and thick solid line is continuous

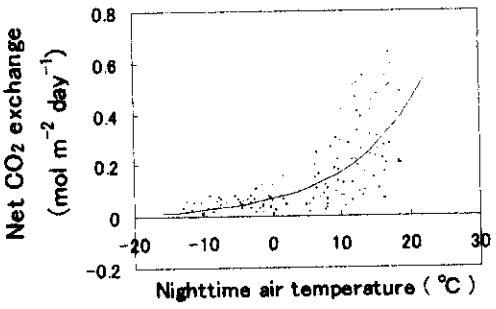

Fig.4. The ecosystem respiration R estimated by the nighttime CO_2 flux measurement from July 1998 to July 1999.

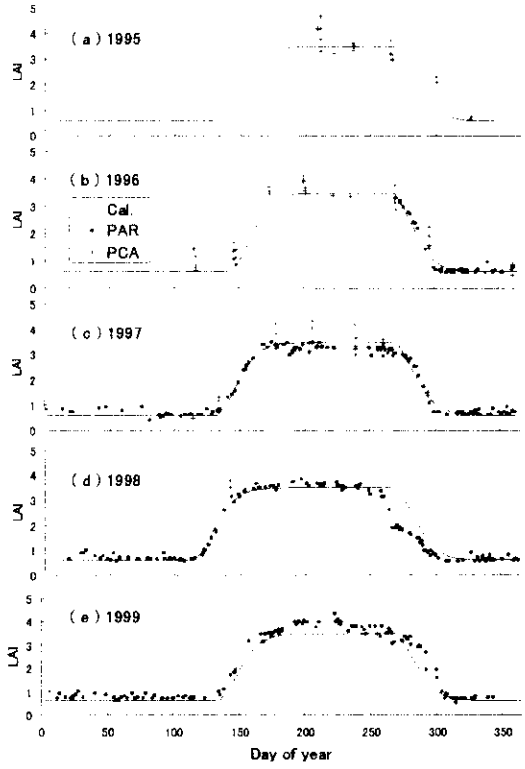

Fig.3. Leaf area index measured by a plant canopy analyzer (PCA), and by the attenuation of photosynthetic active radiation (PAR) from 1995 to 1999. Data include trunk and branch area.

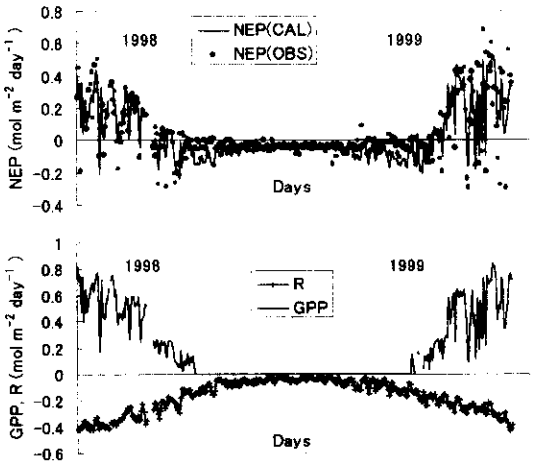

Fig.5. Seasonal changes in observed and calculated NEP, and calculated GPP and R from 1998 to 1999.